Distribution of spectral weight in a system with disordered stripes

M. Granath, V. Oganesyan, D. Orgad, and S. A. Kivelson
Department of Physics, UCLA, Los Angeles, California 90095
(Received 14 September 2001; published 10 April 2002)

The ''band structure'' of a disordered stripe array is computed and compared, at a qualitative level, to angle-resolved photoemission experiments on cuprate high-temperature superconductors. The low-energy states are found to be strongly localized transverse to the stripe direction, so the electron dynamics is strictly one dimensional (along the stripe). Despite this, aspects of the two dimensional band-structure Fermi surface are still vividly apparent.

DOI: 10.1103/PhysRevB.65.184501 PACS number(s): 74.20.−z, 74.25.Jb, 74.72.−h

I. INTRODUCTION

There is strong evidence, in part based on careful analysis of single-particle spectral functions deduced from angle resolved photoemission (ARPES), that the normal state of high-temperature superconductors is not a conventional Fermi liquid. At the same time, there is clear evidence that in some, and possibly in all of these materials, there are local, self-organized quasi-one-dimensional structures, ''stripes,'' which substantially affect the electron dynamics. Many striking features of the ARPES spectrum have a natural interpretation in terms of an electronic structure dominated by stripes.[1–6]

One such feature, which is reproduced in Fig. 1, is that the low-energy spectral weight lies predominantly in regions of the Brillouin zone (BZ) in the vicinity of the $(\pm\pi,0)$ and $(0,\pm\pi)$ points. (These are often referred to as the ''antinodal regions,'' as this is where the maximum in the *d*-wave superconducting gap occurs.) These regions have very straight boundaries which run parallel to the momentum axes, and are displaced by approximately $\pm\pi/4$ from them. This spectral weight has been interpreted in terms of quarter filled stripes (so $k_F=\pi/4$) along the *a* and *b* directions of the lattice.[1,4,7]

However, a number of features of the ARPES data are inconsistent with the most naive picture of an array of strictly one-dimensional quarter-filled stripes. Of these, the most obvious is the occurrence of features, especially in the ''nodal regions'' of the BZ [around $(\pm\pi/2,\pm\pi/2)$], which are reminiscent of the underlying, two-dimensional band structure. An example is the appearance of low-energy spectral weight along segments parallel to the lines connecting the antinodal points in $La_{2-x}Sr_xCuO_4$ (LSCO) and $La_{1.6-x}Nd_{0.4}Sr_xCuO_4$ (LNSCO). A similar signature also appears in Pb-doped $Bi_2Sr_2CaCu_2O_{8+\delta}$ (BSCCO), as shown in Fig. 1.

It is the principal purpose of this paper to elucidate how this apparently two-dimensional structure arises naturally from a slightly more sophisticated analysis of the band-structure of a stripy system. In doing so we extend the initial work of Ref. 1, and complement a recent study of the effects of realistic band parameters on the spectrum by Fleck, Pavarini, and Andersen.[8] We show that a system can exhibit what seems to be a Fermi surface of a two-dimensional metal despite the fact that the *dynamics* of its low-energy electrons is entirely one dimensional. This conclusion holds even in the presence of interactions that preclude any quasiparticle-like description of the system. Under such conditions although the low-energy features in momentum space are sharp, the spectral function, considered as function of energy for fixed momentum, can be broad.[6,9]

Our results are easily summarized. We have computed the band-structure of electrons in the potential generated by a typical configuration of the ''slow'' collective fields that define the stripe order. (The explicit Hamiltonian is presented in Sec. II.) Figures 2 and 3 depict the $\vec{k}$-space distribution of low-energy spectral intensity in the first BZ for disordered and ordered arrays of parallel stripes, respectively. In both cases most of the low-energy spectral weight is concentrated in the antinodal regions. However, while the ordered stripe array exhibits a spectral gap in the nodal region, the disordered array has low-energy weight there, much like that seen in experiment.

We picture the disordered array as being a ''snapshot'' of a ''fluctuating stripe array,'' although it could also reflect the effect of quenched disorder. The low-energy electronic states that are responsible for its spectral map, shown in Fig. 2, lie within the Mott gap. They are bound states that decay exponentially in the direction perpendicular to the stripes. However, they are extended along the stripes, so the low energy electron dynamics is strictly one-dimensional. The resulting band structure, which is shown in Fig. 5, is, to a good approximation, a superposition of the band structures of single isolated stripes and of small clusters (typically pairs) of proximate stripes.

The band structure and spectral distribution of a single stripe are shown in Figs. 6 and 7. Here the fact that the electron wavefunctions in the gap have a non-negligible extent transverse to the stripe can be seen to produce an image of the full two-dimensional band structure. However, as is apparent from the spectrum, unless an isolated stripe is nearly half-filled (which is physically implausible), it will not have any low-energy spectral weight near $(\pi/2,\pi/2)$. This is the reason for the absence of spectral weight in the nodal region of the ordered array since its wave functions are Bloch states constructed from single stripe bound states.

In the disordered array of stripes, the spectral weight in the nodal regions originates primarily from anomalously close pairs of stripes. This is demonstrated in Figs. 9 and 10, which show that for an isolated bistripe, there is low-energy

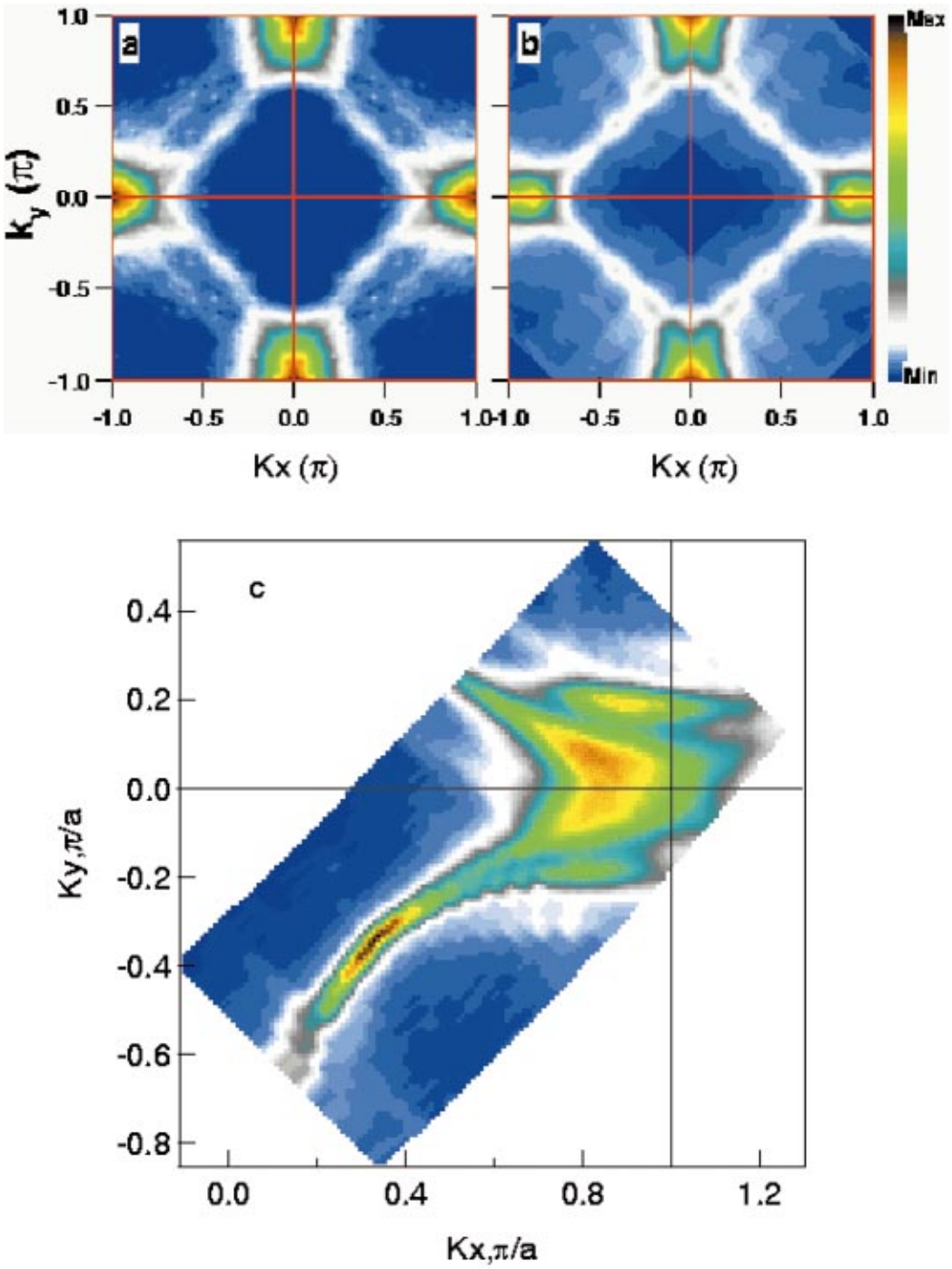

FIG. 1. (Color) Distribution of low-energy spectral weight in the first Brillouin zone as measured by ARPES for various cuprates. The spectral weight was integrated over an energy window of 30 meV below the Fermi energy. Results are shown for (a) $La_{1.6-x}Nd_{0.4}Sr_xCuO_4$ ($x=0.15$) measured at 15 K (from Ref. 7), (b) $La_{2-x}Sr_xCuO_4$ ($x=0.15$) measured at 15 K (from Ref. 7), and (c) overdoped Pb-doped $Bi_2Sr_2CaCu_2O_{8+\delta}$ ($T_c=70$ K) measured at 20 K (from Ref.11).

spectral weight in the vicinity of $(\pi/2,\pi/2)$, even when the stripes are roughly quarter filled. The idea that the intensity of the nodal spectral weight is related to the degree of stripe disorder[7] conforms with the experimental finding (see Fig. 1) of more pronounced Fermi segments in the nodal direction in optimally doped LSCO, where the stripes do not statically order, than in LNSCO, where long-range stripe order is seen in neutron diffraction.[10] Several other experimental observations can be understood in terms of our results, as discussed in Sec. VI.

When residual interactions between electrons on a stripe are considered, each noninteracting localized band gives rise to a one-dimensional Luttinger liquid. As in the noninteracting case the two-dimensional $\vec{k}$ space structure, and especially the Fermi surface, remain prominent features of the low-energy spectral response. However, along a cut in the

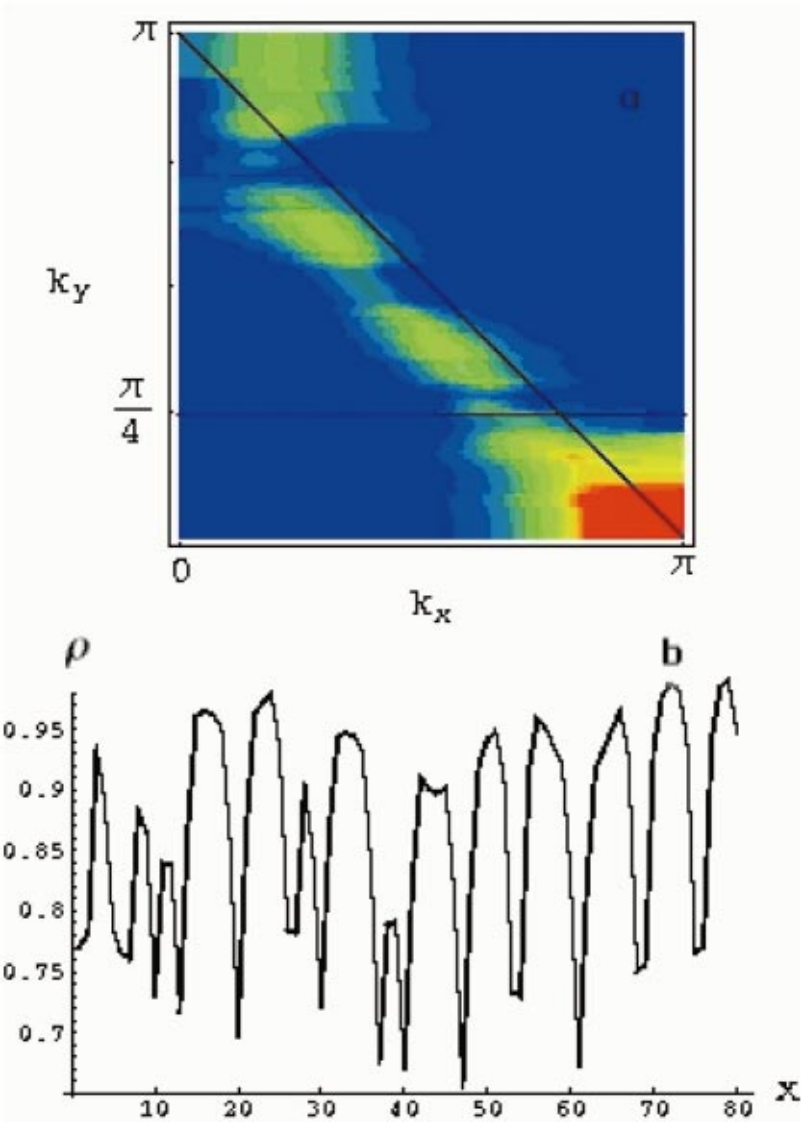

FIG. 2. (Color) (a) The low-energy spectral weight in the first quadrant of the Brillouin zone integrated over an energy interval $\Delta\omega=0.2$ below μ for a disordered stripe array with mean spacings $l=4$ and $m=1$ at $\delta=1/8$ doping. The system size is 320×320 and the amplitude color is coded from blue through green to red, as in Fig. 1. (b) Typical electron density profile of the array as a function of x (perpendicular to the stripe axis). While some of the dips correspond to stripe positions, others, such as the one at $x\approx53$, correspond to bistripes. Thus, in comparison to Fig. 3, below, the density of dips is smaller although the density of stripes is the same.

BZ perpendicular to the Fermi surface, the spectral function mimics Luttinger-liquid behavior. (See, e.g., the behavior along the nodal direction in Fig. 11.) This justifies the application of one-dimensional physics along directions that are not necessarily aligned with the stripes, as recently done in Ref. 6.

It is important to stress that we view the present results as reliable for exploring the qualitative effects of stripes on electronic structure, but not as a realistic study of the cuprate superconductors. The parameters in our model have not been carefully adjusted to optimize any sort of fit to the data. We have certainly not included any ''realistic'' band-structure effects, such as second neighbor hopping, t', nor, except in Sec. V, considered any strong correlation effects, other than the stripes themselves. Phonons, dynamical stripe fluctuations, effects of transverse deformations of the stripe potential, dynamical magnetic fluctuations, and all other forms of static or dynamical disorder are neglected in our calculations. They will all certainly have important consequences for the details of the measured electronic structures. However, it should also be stressed that, throughout this paper, we will be concerned with intermediate energies and length scales. Thus, for our purposes, the distinction between long-range and mesoscale stripe order, and between static and fluctuating stripes is *unimportant*, although of course these distinctions are essential at low energies and long wave-lengths.

II. MODEL

Since high-temperature superconductors are doped antiferromagnets, it is reasonable to expect slow fluctuations of a collective field representing the local staggered magnetization. One can think of this field as resulting from a Hubbard-Stratonovich transformation of the interacting many-body problem. However, we do not solve a Hartree-Fock theory for this field, i.e., we do not find the configuration that minimizes the Hartree-Fock energy. Instead we take as a minimal model a set of non-interacting electrons on a square lattice interacting with a static, staggered field which represents a characteristic ''snapshot'' of the field configuration,

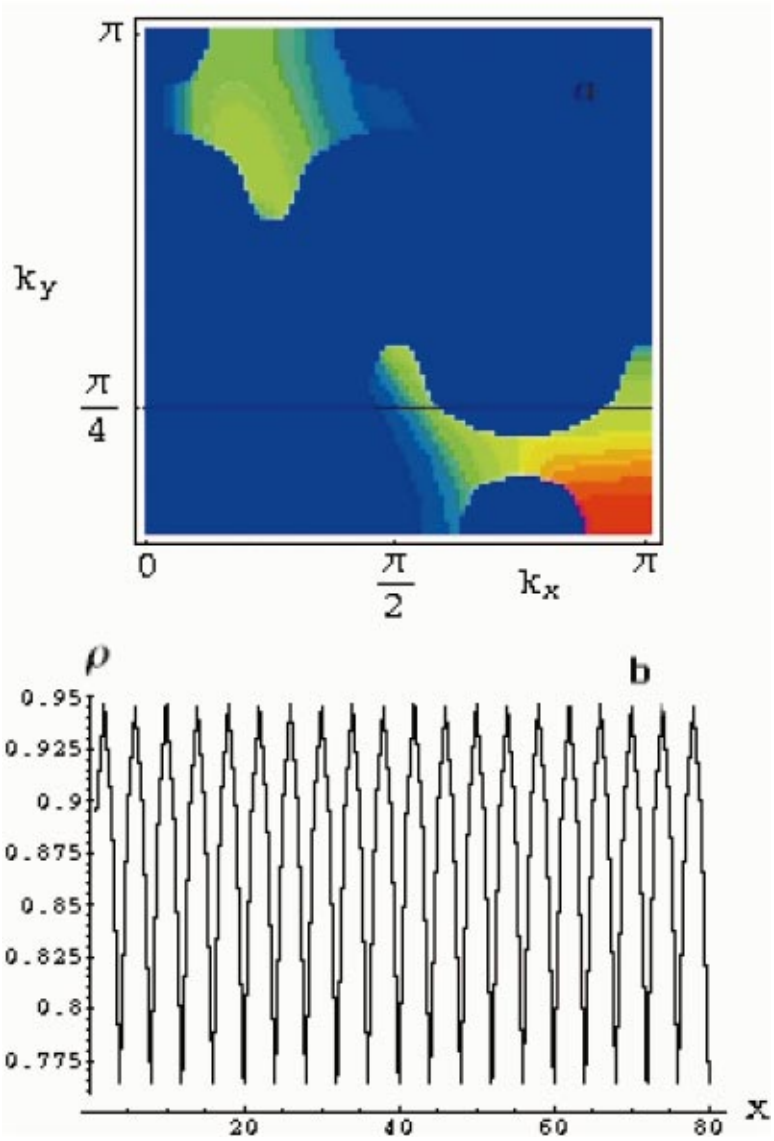

FIG. 3. (Color) Same as in Fig. 2, but for an ordered stripe array with $l=4$, $\delta=1/8$, and $\Delta\omega=0.2$.

$$H=-\sum_{x,y,\sigma}(c^{\dagger}_{x,y,\sigma}c_{x+1,y,\sigma}+c^{\dagger}_{x,y,\sigma}c_{x,y+1,\sigma}+\text{H.c.})$$

$$+\sum_{x,y,\sigma}\sigma(-1)^{x+y}m(x,y)c^{\dagger}_{x,y,\sigma}c_{x,y,\sigma}, \qquad (1)$$

where $c_{x,y,\sigma}$ is the electron destruction operator at site (x,y) and spin $\sigma=\pm$, and we have chosen units such that the hopping matrix element and the lattice constant equal 1. Specifically, we consider the simplest possible ansatz to represent stripe configurations in which

$$m(x,y)=m\prod_{x_s}\Theta(x-x_s), \qquad (2)$$

where m is a constant, $\{x_s\}$ are a given set of positions of antiphase domain walls, and where Θ is the antisymmetric step-function: $\Theta(x)=-\Theta(-x)=1$ for $x>0$ and $\Theta(0)=0$. This corresponds to an array of perfectly straight, site-centered stripes of width 1 oriented in the y direction. Depending on the choice of the set $\{x_s\}$ the potential can either be regular or disordered in the transverse (x) direction.

Some features of the solution below do depend on details of this choice, such as whether the stripes are site or bond centered, whether they are of width 1 or wider, whether we include an additional collective field that couples to the charge density,[1] etc.; effects that we have explored to some extent. However, the important qualitative physics is apparent in this simplest of models, so we only report results for this model. Two more serious omissions, which are beyond the scope of the present paper, are the neglect of effects of the dynamical character of the collective fields, and the neglect of any shape deformations of the stripe order. The latter approximation implies that the electronic states are Bloch waves in the y direction, with a wave vector k_y, which is conserved mod π (due to the presence of the staggered field).

Without the domain walls the system has an energy gap of magnitude $2m$, and two bands with energies $E=\pm\sqrt{m^2+\epsilon^2}$, with $\epsilon=-2[\cos(k_x)+\cos(k_y)]$. An isolated domain wall generates midgap states which are localized in

the direction orthogonal to the wall, as shown analytically below.

For an array of domain walls, it would be exceedingly difficult to find analytical solutions for the midgap states. Instead we diagonalize such systems numerically for a given realization of the model. In each case, we take $m=1$ which corresponds to an ''intermediate coupling'' value of the ratio of the energy gap to the bandwidth of $2/8=1/4$. We study systems with finite width L_x in the x direction, where typically $L_x=320$; according to all tests we have applied, this is large enough to eliminate most finite size effects. Since k_y is a good quantum number, the only place the finite size in the y direction enters our calculations is when we perform sums over k_y; here, it is easy to show that the system sizes we have considered, $L_y=320$, are more than adequate to eliminate finite-size effects.

III. BAND STRUCTURE OF A STRIPE ARRAY

In this section, we consider the spectral weight distribution and band structure of a stripe array. If one ignores details concerning the matrix elements describing the photoexcitation process one can infer directly the single-particle spectral function, $A(\vec{k},\omega)$, from ARPES. For noninteracting electrons, $A(\vec{k},\omega)$ can be expressed in terms of the exact single-particle energy eigenstates $\Psi_\alpha(\vec{r})$ and energies E_α:

$$A(\vec{k},\omega)=(L_xL_y)^{-1}\sum_{\vec{r},\vec{r}'} e^{i\vec{k}\cdot(\vec{r}-\vec{r}')}\tilde{A}(\vec{r},\vec{r}',\omega),$$

$$\tilde{A}(\vec{r},\vec{r}',\omega)=\sum_\alpha \Psi_\alpha(\vec{r})\Psi_\alpha(\vec{r}')\,\delta(\omega-E_\alpha). \qquad (3)$$

In order to characterize the momentum distribution of the low-energy spectral weight and reveal features such as the Fermi surface, it is appropriate to integrate the spectral function over a narrow energy window below the chemical potential μ:

$$I(\vec{k})=\int_{\mu-\Delta\omega}^{\mu} A(\vec{k},\omega)\,d\omega. \qquad (4)$$

The experimental data in Fig. 1, and the theoretical results in later figures are expressed in this way.

In Fig. 3 we report results for an ordered array with a spacing between stripes of $l=4$. In Fig. 2, we do the same for an array with a distribution of stripe spacings chosen randomly between 1 and 7, i.e., a flat distribution with mean $l=4$. In both cases, we have fixed μ such that the average electron density per site is $1-\delta$ where $\delta=1/2l$. (δ is known as the density of ''doped holes.'') This corresponds *on the average* to quarter-filled stripes, such that for $l=4$ we obtain $\delta=1/8$. In these figures, we have chosen $\Delta\omega=0.2$, but the qualitative character of the distribution is not highly sensitive to this choice. The data for the disordered array is for a given realization of the stripe distribution, but the system is large enough that the results are self averaging in the sense that the corresponding figures look similar to the eye for different realizations.

Clearly, a number of salient features of the low-energy spectral weight of these various stripe arrays are reminiscent of those measured in ARPES. In particular the disordered array (Fig. 2) looks strikingly like the corresponding spectrum in LSCO. In both cases, most of the spectral weight is in a broad, flat region close to the $(\pi,0)$ point with a fainter image near $(0,\pi)$. For the ordered array this exhausts the low-energy spectral weight, but for the disordered array, as in the experiments, a small amount of spectral weight lies along what would have been the band-structure Fermi surface in the nodal region. (Of course, in order to compare the results more closely with the ARPES measurements we should symmetrize these results around $k_y=k_x$ to allow for stripes running in both directions in different domains.)

These results demonstrate that two-dimensional structures, including an apparent Fermi surface, can appear in the ARPES data of a system which is dynamically one-dimensional. It is also noteworthy that y-directed stripes not only lead to substantial low-energy spectral weight in the antinodal region near $(0,\pi)$, as naively expected, but also in the reciprocal region, near $(\pi,0)$, as well. (This observation is important in systems with macroscopic stripe orientational order, including, potentially, $YBa_2Cu_3O_{7-\delta}$.[12] We also note that for the ordered array, there are oscillations in the spectral weight as a function of k_x. It is apparent from Fig. 3 that these oscillations reflect the periodicity of the array ($2\pi/4=\pi/2$ in this case. We have checked[13] that for longer period arrays, for example with $l=6$, the period of these oscillations shifts accordingly.) That such oscillations have been observed in LNSCO[4] further corroborates the stripe interpretation of the results.

We have also calculated the electronic density distributions of the disordered and ordered arrays and they are shown next to the spectral maps in Figs. 2 and 3. We see that in the ordered case, the density modulations have the same periodicity as the stripe potential, but in the disordered array, the mean spacing between troughs (or peaks) of the density is larger than the mean spacing between stripes. This reflects the fact that only a single density depression occurs where two stripes are close together. To demonstrate this fact, and to make a connection with neutron-diffraction experiments, we have computed structure factors from the Fourier transforms of the densities of electronic charge (ρ) and z-spin component of the spin (S_z). For the ordered array of period 4 the charge signal is strongly peaked at $k_x=0$ with a small satellite at $k_x=\pi/2$ and the spin signal is peaked at $k_x=3\pi/4$ and $k_x=5\pi/4$. For the disordered array the charge and spin peaks are shifted toward $k_x=0$ and $k_x=\pi$ respectively. In Fig. 4 we show the Fourier transform of the autocorrelation function of the random field m. (We show the results for m rather than for S_z, because it can be computed for very large arrays, where the result is self-averaging. However, we have verified that the two quantities give similar results.[13]) The fact that for the disordered array, the spin peaks are not only broadened, but are shifted toward the (π,π) point seems to be generic behavior for disordered arrays.

Since k_y is still a good quantum number, we can still talk about a (one-dimensional) band structure of the disordered

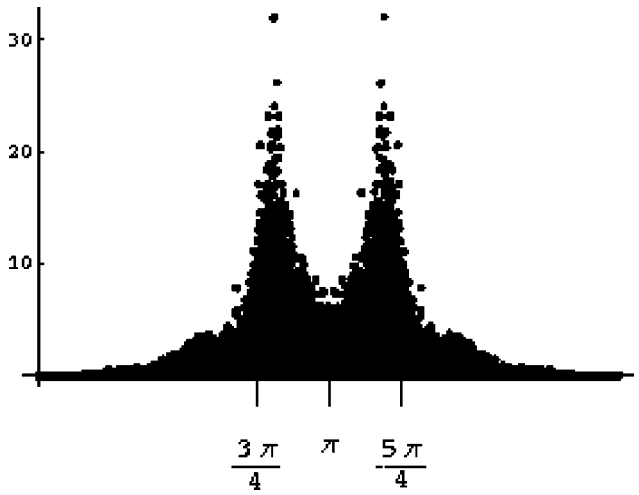

FIG. 4. The squared magnitude of the Fourier transform of the field $m(x,y)$ for a disordered array of size $L_x=100{,}000$. This quantity is proportional to the spin-spin correlation function measured by neutron scattering.

array, as shown in Fig. 5. However, as there are precisely $2L_x$ bands, this figure becomes rather dense for a large number of stripes, so we have purposely reduced the system size to $L_x=80$ and the energy window to $|E|<2$ for graphical clarity. We devote Sec. IV to a closer examination of this band-structure.

Because for each value of k_y, the effective Hamiltonian is that of a one-dimensional disordered system in the x direction, we know *a priori* that all the states are exponentially localized transverse to the stripes. However, for the states that lie within the Mott gap, $|E|<m=1$, one might expect the states to be highly localized in the neighborhood of one or two stripes, while for $|E|>m=1$, the states are more likely extended scattering states, that are only weakly localized. That this expectation is realized can be seen in at least three ways. It is clear from Fig. 5 that there is a dense set of states at $E>m=1$, whereas for $E<m=1$ there is a spider web of identifiable one-dimensional bands; the discreteness of these bands is a reflection of their large degree of localization in the transverse direction. By plotting the states in

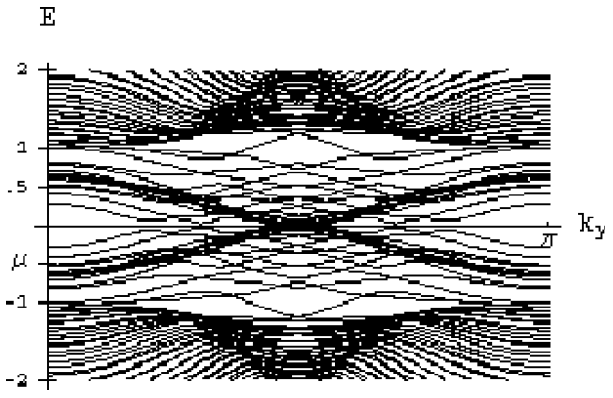

FIG. 5. Band structure of a disordered array with mean stripe spacing $l=4$ and $m=1$. μ is the $T=0$ chemical potential for a density of doped holes $\delta=1/8$. The system size is 80×320.

real space along x, we have confirmed that all the states in the gap decay exponentially in a few lattice constants, whereas the scattering states are essentially delocalized. Finally, we have computed the participation ratio $P_\alpha \equiv \Sigma_{\vec{r}}|\Psi_\alpha(\vec{r})|^4 \approx (2\xi)^{-1}$, where ξ is the localization length. For a system of size 320×320, we find P's for the states with $|E|>m$ of order $P\sim1/100$ (which might become even smaller for larger system sizes), while for $|E|<m$, typically $P\approx0.1$–0.25. For moderate doping δ the Fermi energy always lies inside the set of highly localized bands. (See, for example, Fig. 5, where the value of the Fermi energy corresponding to $\delta=1/8$ is indicated.) It is clear that all of the spectral weight shown in Fig. 2 comes from these localized, and hence dynamically entirely one-dimensional states.

IV. ISOLATED STRIPES AND BISTRIPES

In order to obtain a better understanding of the nature of the localized states and how they give rise to the very characteristic two-dimensional distribution of spectral weight, we look at some simpler problems consisting of a single or a pair of proximate domain walls. Consider the situation in which the defects, i.e., one or more stripes, are confined to a region about $x=0$. It is straightforward to explicitly write the wave functions for fixed k_y in the asymptotic regions to the left and right of the defect; the eigenvalue problem is then solved by matching these solutions across the defect region. For $|E|<m$, the asymptotic states are exponentially falling functions of x. For instance, to the right of the defect, Hamiltonian (1) is diagonalized by

$$\phi_{k_y}(x,y)=e^{-\kappa x}e^{i(qx+k_y y)}[1+e^{i\alpha}e^{i\pi(x+y)}], \tag{5}$$

where the quantities κ, q, and α are the implicit functions of k_y and the energy E which (for $\sigma=1$) satisfy

$$0=\cos(q)\cosh(\kappa)+\cos(k_y), \tag{6}$$

$$E^2=m^2-4\sinh^2(\kappa)\sin^2(q), \tag{7}$$

$$e^{i\alpha}=[E+2i\sinh(\kappa)\sin(q)]/m. \tag{8}$$

It follows from Eqs. (6)–(8) that if Eq. (5) is a solution then so is Eq. (5) with $q\to-q, \alpha\to-\alpha$, and the same energy. Thus the total wave function $\Phi_{k_y}(x,y)$ is a linear superposition of the two. To the left of the defect the same equations hold after substituting $\kappa\to-\kappa$ and, in the case of an antiphase defect, $m\to-m$. A fourth equation, which depends on the nature of the defect, is obtained by integrating the Schrödinger equation across the defect region, and defines the eigenvalue problem $E=E(k_y)$. (If the defect region is sufficiently broad, there may be multiple solutions to the eigenvalue equation, corresponding to multiple midgap bands.)

Much of the interesting physics is already implicit in these relations. The distribution of spectral weight in the two-dimensional BZ associated with a state of given crystal momentum k_y is given by $|\Psi_{k_y}(k_x)|^2$, where Ψ is the Fourier transform of Φ. Clearly, this weight is peaked near $k_x=q(k_y)$ in a region of width $\Delta k_x\approx\kappa(k_y)$. For small κ, Eq.

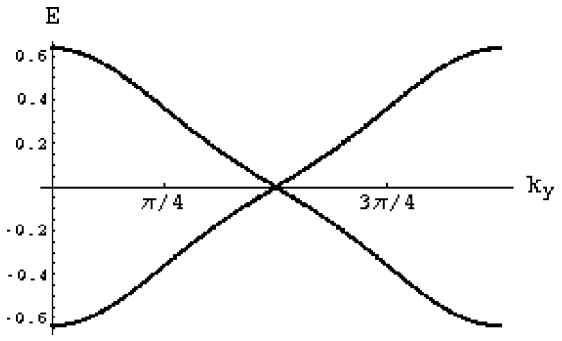

FIG. 6. Dispersion $E(k_y)$ of the bound states of a single antiphase domain wall with $m=1$.

(6) implies that $q(k_y)$ simply traces out the underlying ''diamond'' Fermi surface given by the unperturbed band-structure.

To be explicit, let us consider the case of a single site-centered antiphase domain wall, $(\downarrow\uparrow\downarrow\uparrow\cdot\downarrow\uparrow\downarrow\uparrow)$ of the type which appears in Eq. (2). In this case, the eigenvalue equation is readily derived:

$$E(k_y)=\pm 2\tanh^2(\kappa)\cos(k_y). \tag{9}$$

The resulting band-structure and spectral weight distribution in the BZ is shown in Figs. 6 and 7. Note that the midgap band has energy zero precisely where $k_y=\pi/2$, so that, for a hole-doped stripe, for which the Fermi energy will certainly lie at negative energies, there will never be low-energy spectral weight at the nodal point. A generic feature of the spectral weight distribution that is apparent in the figure is the fact that the negative-energy states have more weight in the lower half of the first quadrant of the BZ than in the upper half. This feature is seen very clearly also in the disordered array problem (Fig. 2).

It is particularly illuminating to examine this result in the small-m limit. The four implicit equations can be solved to leading order in m to obtain (for $0<k_y<\pi$)

$$q(k_y)=\pi-k_y, \tag{10}$$

$$\kappa(k_y)=\frac{m}{2\sin(k_y)}, \tag{11}$$

$$E(k_y)=\pm 2\kappa^2(k_y)\cos(k_y). \tag{12}$$

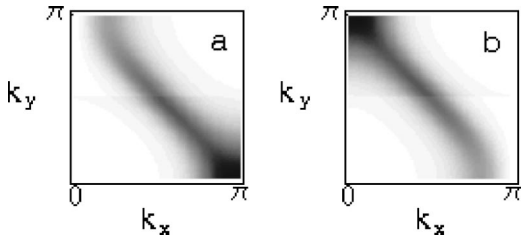

FIG. 7. Integrated spectral weight over all negative- (a) and positive- (b) energy bound states of a single antiphase domain wall with $m=1$. The apparent discontinuity across $k_y=\pi/2$ is due to the band crossing.

As advertised, $q(k_y)$ precisely traces out the diamond Fermi surface. $\kappa^{-1}(k_y)\sim v_F(k_y)/m$ is the extent of the wave function in real space, implying that $|\Psi_{k_y}(k_x)|^2$ is quite sharply peaked near $k_x=q(k_y)$ in the nodal regions, where the Fermi velocity v_F is large, and is much more diffused in the antinodal regions, where $v_F\to 0$. (Where $v_F=0$, the expression for κ breaks down and we find $\kappa\sim\sqrt{m}$.) These features are, to a large extent, independent of the nature of the defect, so long as m is not too large. It is also worth noting that the energy width of the midgap band is of order m^2, although the gap itself is $2m$, and hence much larger.

The single antiphase domain-wall solution captures most of the general features of the array of domain walls: The spectral weight is concentrated about the diamond Fermi surface, it is largest in a broad antinodal region, and is larger in the lower half than in the upper half of the BZ quadrant. Indeed, the low-energy spectral distribution of the ordered stripe arrays is, to a first approximation, simply the sum of contributions of isolated stripes, even when the stripe spacing is only four lattice constants.

However, the disordered stripe array is not simply a superposition of single-wall states, especially in the nodal region. In fact, while it is clear from the band structure of the disordered array shown in Fig. 5, that a large fraction of the midgap bands are very similar to the mid-gap band of a single isolated stripe (Fig. 6), there are other bands, especially those that dominate the spectrum at $k_y=\pi/2$ and E near μ, that look very different.

Guided by the observation that the nodal weight is missing for an ordered array, it is reasonable to assume that this feature is related to local configurations with two or more domain walls in close proximity. Consider, therefore, the problem of two anti-phase domain walls in close proximity. Clearly, the statement of proximity is related to the decay length $\xi=1/\kappa$ of the single-domain-wall problem. If the distance between the walls is greater than ξ, the walls can be considered independent, while for smaller distances they interfere. For $m=1$ we find $1/\kappa\approx 2$ and only weakly dependent on k_y, implying that domain walls separated by more than two sites are roughly independent. Figure 8 shows the energy spectrum for the bound states of two antiphase domain walls separated by one site. The spectrum is gapped and it is clear that doping such a system can give rise to low-energy spectral weight around $k_y=\pi/2$. In Fig. 9 we repeat the same calculation for two proximate stripes.

Particularly interesting is the distribution of spectral weight in momentum space for this system, as shown in Fig. 10. As with the single-wall problem, the weight hovers around the band-structure Fermi surface, but with the distinct feature that the weight of the negative-energy states is shifted toward the zone center, whereas the positive-energy states are shifted toward the (π,π) point. We find that the magnitude of this shift increases with m. Intuitively it is of course not surprising that the negative-energy states are shifted towards the zone center where the tight-binding energies are lower, and conversely for the positive energy states.

V. INCLUDING INTERACTIONS

So far we have been concerned with the distribution of spectral weight in the noninteracting model defined in Eq.

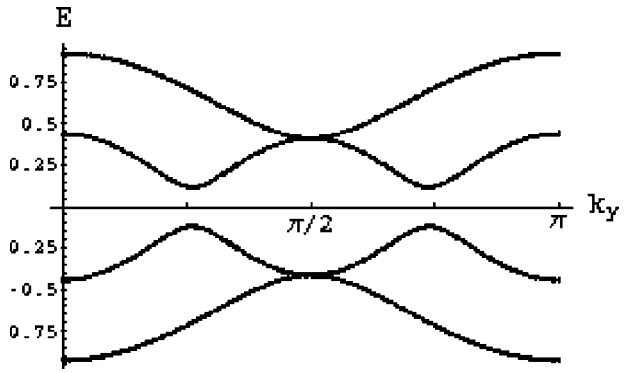

FIG. 8. Spectrum $E(k_y)$ of the bound states of an effective in-phase domain wall consisting of two one-site wide antiphase domain walls one site apart ($\uparrow\downarrow\uparrow\downarrow\cdot\uparrow\cdot\downarrow\uparrow\uparrow\downarrow$), with $m=1$.

(1), when holes are introduced into its single-particle levels. Including the effects of interactions between electrons in a doped stripe is a natural extension of this model. In the following we consider this issue for the case of the disordered stripe array.

To the extent that the localized bands shown in Fig. 5 can be considered as independent we may calculate the low-energy and long-wavelength spectral response of the system as a sum over interacting Luttinger-liquid contributions $A_{1d}(k,\omega)$:

$$A(\vec{k},\omega)=\sum_{k_F} |\Psi_{k_F}(k_x)|^2 A_{1d}[k_y-k_F,\omega;\gamma(k_F)]. \quad (13)$$

Here the sum runs over the localized bands that cross the Fermi energy. Every crossing point is a Fermi point $k_F \equiv \vec{k}_F\cdot\hat{y}$ for the one-dimensional channel defined by the band. Each channel is also characterized by the k_x profile of its wave function $\Psi_{k_F}(k_x)$ and its Luttinger parameters $K_{c,s}$ and velocities $v_{c,s}$ which are collectively denoted as $\gamma(k_F)$ in (13).

The evaluation of spectral function (13) simplifies in the small-m limit where the spectral weight is concentrated (within a width of order m) along the diagonal connecting the antinodal points and is roughly constant. The total spectral function is then proportional to $A_{1d}(k_x+k_y-\pi,\omega;\gamma)$, where we have assumed that γ is the same for all bands. As

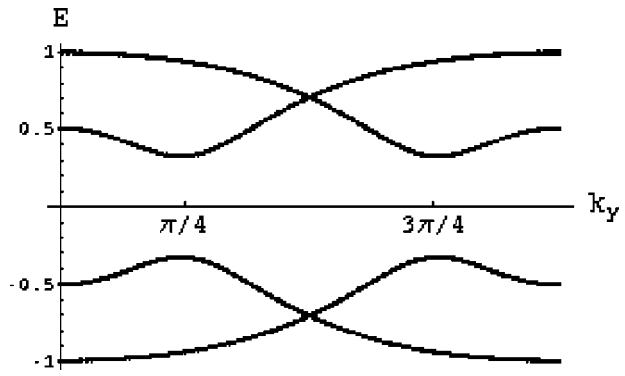

FIG. 9. Spectrum $E(k_y)$ of the bound states of a two-site wide in-phase domain wall ($\uparrow\downarrow\uparrow\downarrow\cdot\cdot\uparrow\downarrow\uparrow\downarrow$) with $m=1$.

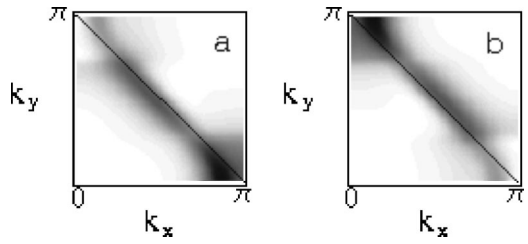

FIG. 10. Integrated spectral weight over all negative- (a) and positive- (b) energy states of an in-phase domain wall consisting of two one-site antiphase domain walls one site apart with $m=1$.

we see, in this case, the spectral function exhibits one-dimensional behavior over the entire BZ. This description is valid as long as the stripe array is sufficiently dilute such that the overlaps between different localized bands are small.

For intermediate values of m performing the convolution in Eq. (13) is difficult, owing to the complicated distribution of the low-energy spectral weight in momentum space. However, the spectral function continues to mimic one-dimensional behavior along directions that are not necessarily aligned with the stripes. To demonstrate this point, we consider the spectral function along a cut in the BZ that runs in the nodal direction [from (0,0) to (π,π)]. Since the zero-temperature $A_{1d}(k-k_F,\omega;\gamma)$ vanishes unless $|\omega| > \min(v_c,v_s)|k-k_F|$,[6] it is clear that the important contribution to $A(\vec{k},\omega)$ along this cut, and at low energies, comes from bands that cross the Fermi energy near $k_y=\pi/2$. Moreover, we have shown that these bands produce a spectral weight that is concentrated along a line parallel to the antidiagonal [$(\pi,0)$ to $(0,\pi)$]. Therefore, for our purpose, we may approximate the spectral distribution by a Lorentzian distribution centered on this line with a half-width at half-maximum of κ. In Fig. 11 we present the spectral function which results from Eq. (13) under the assumption of such a weight distribution.

The spectral function in Fig. 11 shows a close resemblance to one-dimensional spectral functions (compare, for example, with Ref. 6). In particular it exhibits a striking dichotomy between sharp momentum distribution curves [(MDC's), cuts at constant ω] and broad energy distribution curves [(EDC's), cuts at constant k], which we believe is a telltale of electron fractionalization.[6] It is interesting to note, however, that $A(\vec{k},\omega)$ in Fig. 11 is smoother than the corresponding zero-temperature one-dimensional spectral function, and does not diverge at $\omega=vk$ for $k<0$ like the latter. This divergency is smeared by the convolution in Eq. (13), and the result is a spectral function that resembles $A_{1d}(k,\omega)$ but at a finite temperature.

The present analysis is the first which combines the remarkable non-Fermi-liquid features of the one-dimensional electron gas with the two-dimensional structure of a Fermi surface. At a qualitative level, it justifies the analysis presented in Ref. 6, in which the measured spectral functions of the high-temperature superconductors was analyzed in terms of the corresponding expressions for a one-dimensional Luttinger liquid. In particular, here we have presented a microscopic rationale, which was missing at the time of that earlier

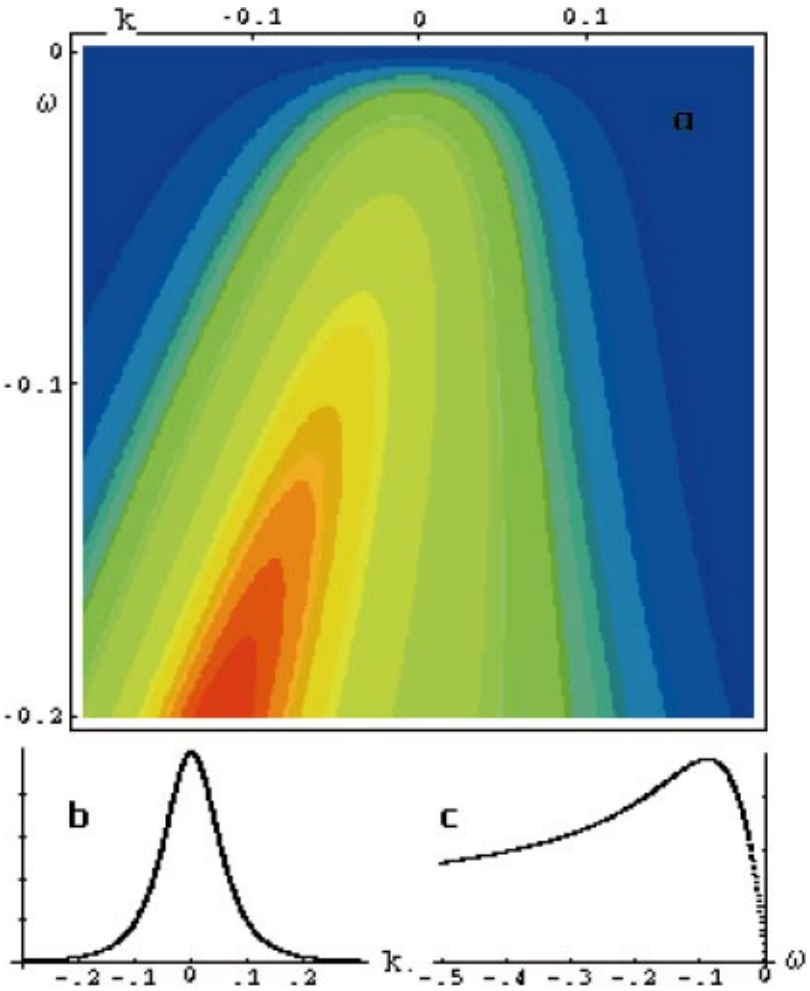

FIG. 11. (Color) (a) The zero-temperature spectral function $A(k,\omega)$ calculated from Eq. (13) assuming a Lorentzian distribution of spectral weight centered on a line parallel to the antidiagonal. Here $v_c=v_s=1$, $K_s=1$, $\gamma_c=(K_c+K_c^{-1}-2)/8=0.3$, and $\kappa=0.5$ (which is what we find for a single stripe with $m=1$). k is measured along the BZ diagonal and relative to the Fermi point near $(\pi/2,\pi/2)$, ω is measured relative to the chemical potential μ. (b) MDC at $\omega=0$, (c) EDC at $k=0$.

work, for the existence of approximate one-dimensional dynamics in the nodal region of the Fermi surface.

VI. FURTHER CONSEQUENCES

In addition to the gross similarities between the experimentally observed spectral functions in LSCO, LNSCO, and BSCCO and those obtained from simple stripe models, there are a number of other aspects of the present results that are potentially relevant to the interpretation of experiment.

A phenomenon that is fairly generally observed in ARPES measurements on high-temperature superconductors is that a sharp quasi-particle-like peak appears in the spectrum in the antinodal regions as the temperature is reduced below T_c. Recent experiments on untwinned $YBa_2Cu_3O_{7-\delta}$ (YBCO) crystals have found that the spectral-weight of this sharp feature exhibits strong anisotropy between the different antinodal regions of the BZ.[12] There are good empirical[14,15] and theoretical[16] reasons to believe that the stripes in this material are partially oriented by the chain potential on the Cu-O planes. Thus a large anisotropy in plane-related features is to be expected. Moreover, we have previously shown[5] that the emergence of such a peak is naturally explained as a dimensional crossover in a quasi-one-dimensional superconductor. However, the presence of low-energy spectral weight in the anti-nodal region transverse to the stripes seems surprising at first. Nevertheless, as noted above, stripes induce low energy spectral weight in both antinodal regions, although with different spectral weights—this is a consequence of strong mixing between states separated by the antiferromagnetic wave vector (π,π). The observed anisotropy is reproduced naturally by the present model—see Fig. 2.

One would generally expect electrons diffracting off an ordered stripe array to exhibit intensity modulations with the corresponding period, as indeed is apparent in the period $\pi/2$ structure seen in Fig. 3. We believe, in agreement with the interpretation proposed by Zhou *et al.*,[4] that this effect has already been seen in ARPES spectra of LNSCO.[4] Since all previous observations of charge-density wave ordering are indirect (e.g., they detect the accompanying lattice distortion density wave), this observation is potentially of more far reaching importance as a method for detecting charge order.

Experiments on both electron and hole-doped cuprates indicate that the chemical potential remains within the Mott gap, and is a remarkably slowly varying function of dopant concentration; instead, new dopant-induced states appear in the gap.[17–19] Of course, this behavior is characteristic of the sort of stripe models envisaged here, in which the density of stripes increases with dopant concentration so as to accommodate the added charges in midgap states. This is a form of ''topological doping''[20] analogous to soliton doping of

polyacetylene.[21] As is the case in polyacetylene, we expect a variety of additional aspects of topological doping to be manifest in experiments on the cuprates, including dopant-induced midgap optical absorption,[1,3] dopant-induced infrared-active phonon modes,[22] etc.

Finally, the observation that the structure factor of a disordered stripe array exhibits incommensurate peaks that are not only broadened by disorder, but also shifted to smaller incommensurability (Fig. 4) may have other interesting implications. Inelastic neutron-scattering experiments in LNSCO,[10] LSCO,[23] and YBCO (Ref. 24) revealed incommensurate magnetic peaks displaced from the antiferromagnetic wave vector, (π,π), by an amount which first grows roughly linearly with doping, but then tends to saturate (typically beyond $\delta=1/8$). This is generally taken as evidence that the concentration stripes, likewise, first increases linearly and then saturates. Our present results suggest that, at least in part, the saturation of the incommensurability may reflect increasingly strong stripe fluctuations, rather than a sudden saturation of the stripe concentration.

ACKNOWLEDGMENTS

We would like to acknowledge helpful discussions with J. W. Allen, P. D. Johnson, J. M. Tranquada and Z.-X. Shen. We thank P. Bogdanov and X. J. Zhou for providing us with their data. M.G. acknowledges support from the Swedish Foundation for International Cooperation in Research and Higher Education (STINT). S.A.K., V.O., and D.O. were supported in part by NSF Grant No. DMR-0110329 and U.S. DOE Grant No. DE-FG03-00ER45798.

[1] M.I. Salkola, V.J. Emery, and S.A. Kivelson, Phys. Rev. Lett. **77**, 155 (1996).

[2] M.G. Zacher, R. Eder, E. Arrigoni, and W. Hanke, Phys. Rev. Lett. **85**, 2585 (2000).

[3] M. Ichioka and K. Machida, J. Phys. Soc. Jpn. **68**, 4020 (1999).

[4] X.J. Zhou, P. Bogdanov, S.A. Kellar, T. Noda, H. Eisaki, S. Uchida, and Z.-X. Shen, Science **286**, 268 (1999).

[5] E.W. Carlson, D. Orgad, S.A. Kivelson, and V.J. Emery, Phys. Rev. B **62**, 3422 (2000).

[6] D. Orgad, S.A. Kivelson, E.W. Carlson, V.J. Emery, X.J. Zhou, and Z.-X. Shen, Phys. Rev. Lett. **86**, 4362 (2001).

[7] X.J. Zhou, T. Yoshida, S.A. Kellar, P.V. Bogdanov, E.D. Lu, A. Lanzara, M. Nakamura, T. Noda, T. Kakeshita, H. Eisaki, S. Uchida, A. Fujimori, Z. Hussain, and Z.-X. Shen, Phys. Rev. Lett. **86**, 5578 (2001).

[8] M. Fleck, E. Pavarini, and O.K. Andersen, cond-mat/0102041 (unpublished).

[9] T. Valla, A.V. Fedorov, P.D. Johnson, Q. Li, G.D. Gu, and N. Koshizuka, Phys. Rev. Lett. **85**, 828 (2000).

[10] J.M. Tranquada, J.D. Axe, N. Ichikawa, A.R. Moodenbaugh, Y. Nakamura, and S. Uchida, Phys. Rev. Lett. **78**, 338 (1997).

[11] P.V. Bogdanov, A. Lanzara, X.J. Zhou, S.A. Kellar, D.L. Feng, E.D. Lu, H. Eisaki, J.-I. Shimoyama, K. Kishio, Z. Hussain, and Z.-X. Shen, Phys. Rev. B **64**, 180505(R) (2001).

[12] D.H. Lu, D.L. Feng, N.P. Armitage, K.M. Shen, A. Damascelli, C. Kim, F. Ronning, Z.-X. Shen, D.A. Bonn, R. Liang, W.N. Hardy, A.I. Rykov, and S. Tajima, Phys. Rev. Lett. **86**, 4370 (2001).

[13] Data files for the figures presented in this paper, as well as additional results mentioned in the text but not presented in the paper, can be found at http://fy.chalmers.se/~mgranath/figures/. In particular, the low-energy spectral distribution for an ordered array of period $l=6$, and the structure factors for S_z and ρ for the disordered array with mean stripe spacing $l=4$ are available there for viewing.

[14] H.A. Mook, P. Dai, F. Doğan, and R.D. Hunt, Nature (London) **404**, 729 (2000).

[15] Y. Ando, K. Segawa, S. Komiya, and A.N. Lavrov, Phys. Rev. Lett. **88**, 137005 (2002).

[16] S.A. Kivelson, E. Fradkin, and V.J. Emery, Nature (London) **393**, 550 (1998).

[17] J.W. Allen, C.G. Olson, M.B. Maple, J.-S. Kang, L.Z. Liu, J.-H. Park, R.O. Anderson, W.P. Ellis, J.T. Markert, Y. Dalichaouch, and R. Liu, Phys. Rev. Lett. **64**, 595 (1990); R.O. Anderson, R. Cleassen, J.W. Allen, C.G. Olson, C. Janowitz, L.Z. Liu, J.-H. Park, M.B. Maple, Y. Dalichaouch, M.C. de Andrade, R.F. Jardim, E.A. Early, S.-J. Oh, and W.P. Ellis, *ibid.* **70**, 3163 (1993).

[18] T. Watanabe, T. Takahashi, S. Suzuki, S. Sato, and H. Katayama-Yoshida, Phys. Rev. B **44**, 5316 (1991).

[19] A. Ino, C. Kim, M. Nakamura, T. Yoshida, T. Mizokawa, Z.-X. Shen, A. Fujimori, T. Kakeshita, H. Eisaki, and S. Uchida, Phys. Rev. B **62**, 4137 (2000).

[20] S.A. Kivelson and V.J. Emery, Synth. Met. **80**, 151 (1996).

[21] For a review, see A.J. Heeger, S.A. Kivelson, J.R. Schrieffer, and W.P. Su, Rev. Mod. Phys. **60**, 781 (1988).

[22] Preliminary evidence of such behavior in very lightly doped LSCO was recently observed by Dumm, Basov, and Ando (private communication).

[23] K. Yamada, C.H. Lee, K. Kurahashi, J. Wada, S. Wakimoto, S. Ueki, H. Kimura, Y. Endoh, S. Hosoya, G. Shirane, R.J. Birgeneau, M. Greven, M.A. Kastner, and Y.J. Kim, Phys. Rev. B **57**, 6165 (1998).

[24] P. Dai, H.A. Mook, R.D. Hunt, and F. Doğan, Phys. Rev. B **63**, 054525 (2001).